

Proton resonances in ^{30}P

R. O. Nelson, E. G. Bilpuch, and C. R. Westerfeldt

*Duke University, Durham, North Carolina**and Triangle Universities Nuclear Laboratory, Duke Station, Durham, North Carolina 27706*

G. E. Mitchell

*North Carolina State University, Raleigh, North Carolina**and Triangle Universities Nuclear Laboratory, Duke Station, Durham, North Carolina 27706*

(Received 14 October 1982)

The $^{29}\text{Si}(p,p)$ and (p,p') differential cross sections were measured in the range $E_p = 1.29\text{--}3.31$ MeV with an overall resolution of 350–400 eV, full width at half maximum. Resonance parameters were extracted for 66 resonances with a multilevel, multichannel R -matrix analysis code; these parameters include resonance energy, total angular momentum, partial elastic and inelastic widths, and channel spin and orbital angular momentum mixing ratios. Analog states were identified, and Coulomb displacement energies and spectroscopic factors are given for seven of these analog states.

<p>NUCLEAR REACTIONS $^{29}\text{Si}(p,p),(p,p')$, $E = 1.29\text{--}3.31$ MeV, measured $\sigma(E,\theta)$. ^{30}P levels deduced J^π, Γ_p, $\Gamma_{p'}$, channel spin mixing l mixing; ^{30}P IAS deduced Coulomb energies, spectroscopic factors. Enriched target, resolution 350–400 eV.</p>

I. INTRODUCTION

Previous high resolution proton resonance studies at the Triangle Universities Nuclear Laboratory (TUNL) have been confined to even-even target nuclei, with emphasis placed first on the fine structure of analog states and later on statistical properties of compound nuclear states. Spin-zero targets were ideally suited for these studies, due in part to analysis simplifications which result when there is only one entrance channel for a given resonance and when only one or two open decay channels contribute significantly. Most of the measurements were performed in the nuclear $1f\text{--}2p$ shell, with some data in the $2s\text{--}1d$ shell.

We should like to extend these measurements to targets with spin. Considering odd-mass targets in the $2s\text{--}1d$ shell avoids the complexities of many open neutron channels and of very high level densities. Although the neutron channel is normally closed for proton bombarding energies of a few MeV, there are usually several open inelastic decay channels and often open alpha channels. The analysis is further complicated by the possibilities of channel spin mixing and of orbital angular momentum mixing. Both broad and very narrow resonances are observed in scattering from these nuclei; thus high resolution is required for the detection and analysis of the small resonances, and a multilevel, multichannel analysis is necessary to fit the broad, interfering levels.

For excitation energies of the compound systems formed in low energy proton scattering, the available spectroscopic information is much more extensive for spin-zero targets than for odd-mass targets.¹ In particular, there is very little good resolution elastic scattering data for odd-mass targets. The detailed spectroscopy possible with odd-mass targets, including channel spin mixing and l mixing, is of interest in its own right. A further motivation is imparted by the significance of channel spin mixing and l mixing for fundamental symmetry tests with resonances. The importance of l mixing for time reversal invariance tests was pointed out by Pearson and Richter² and demonstrated in a test of detailed balance by Driller *et al.*³ Parity mixing for compound states is discussed by Sushkov and Flambaum⁴ and has been demonstrated experimentally by Alfimov *et al.*⁵ The significance of channel spin mixing is shown in their results. Time reversal invariance tests utilizing polarization from resonances have been proposed by Barker and Ferdous.⁶ Improvement of the spectroscopy in this mass region, particularly for channel spin mixing and l mixing, is necessary to select resonances which are best suited for symmetry tests.

The nucleus ^{29}Si was chosen for a first study of odd-mass targets because the most information was available from previous good resolution experiments, the level density was relatively low, and the ground state spin $\frac{1}{2}$ introduces less complexity than higher

spins. The $^{29}\text{Si}(p,p)$ reaction had been studied previously with poor resolution by Storizhko and Popov,⁷ L'vov *et al.*,⁸ and with better resolution by Poirier *et al.*⁸ and Hemskey *et al.*¹⁰

In the present experiment the excitation functions for $^{29}\text{Si}(p,p)$, (p,p_1) , and (p,p_2) were measured from 1.29, 2.40, and 3.09 MeV, respectively, to 3.31 MeV. The overall resolution was 350 to 400 eV (FWHM). Sixty-six resonances were observed and fit; twenty-eight had not previously been fit and five of these had not been observed as resonances in elastic scattering. The experimental procedure is described in Sec. II while details of the analysis are given in Sec. III. Results of the analysis are presented in Sec. IV and analog states are discussed in Sec. V.

II. PROCEDURE

The experiment was performed with the 3 MV Van de Graaff and associated high resolution system at TUNL. This system has been described elsewhere.^{11,12} The targets consisted of 0.8 to 1.3 $\mu\text{g}/\text{cm}^2$ Si enriched to 95% in ^{29}Si , evaporated onto 2 $\mu\text{g}/\text{cm}^2$ collodion coated carbon foils. The vacuum evaporation was performed with a closed Ta boat and Ta powder as a reducing agent. This method appeared to give lower oxygen contamination than the electron gun method, and due to evaporation at temperatures just above the melting point of SiO_2 the Ta contamination was also slight.

Surface barrier detectors placed at laboratory angles of 90°, 105°, 135°, and 160° detected the scattered protons. Dead time and pulse pileup problems due to the strong $^{12}\text{C}(p,p)$ resonances near $E_p=1.7$ MeV were minimized by electronically gating the carbon peak out of the spectra, and by using very thin target backings. In addition data were buffered in a CAMAC module and transferred directly to computer memory to reduce system dead time. Data were taken in energy steps of 100 eV over small resonances and in steps less than 500 eV over very large resonances and off resonance. Typical beam currents of 3 to 6 μA with counting times of 30 to 60 sec maintained 1% counting statistics in the off resonance yield. Absolute energy calibrations¹³ were based on the $^7\text{Li}(p,n)$ threshold at 1.8806 MeV and the $^{13}\text{C}(p,n)$ threshold at 3.2357 MeV. Absolute energies are believed accurate to ± 3 keV, while relative energies over a small energy range are reproducible to a few hundred eV. The contribution from broad resonances¹⁴ in the ^{28}Si contaminant was calculated and subtracted from the cross section. This contamination arose from both the isotopic material (4.4%) and from natural silicon from the target preparation. The ^{28}Si fraction was experimentally determined to be 7%. In addition an

f -wave analog state¹⁵ at $E_p=2.187$ MeV from the 0.36% ^{30}Si contaminant was observed in the 160° cross section.

III. ANALYSIS

For protons elastically scattered from a spin $\frac{1}{2}$ target the channel spins are $s=0$ and 1. Natural parity resonances allow only channel spin mixing, while unnatural parity resonances allow only l mixing. The elastic scattering channel spin mixing ratio is defined as

$$\xi = \Gamma_{p,s=1,l} / [\Gamma_{p,s=0,l} + \Gamma_{p,s=1,l}], \quad (1)$$

and the l mixing ratio is

$$\epsilon = \pm [\Gamma_{p,s=1,l+2} / \Gamma_{p,s=1,l}]^{1/2}, \quad (2)$$

where $\Gamma_{p,s,l}$ is the laboratory width for elastic scattering of the l th partial wave with channel spin s . Thus, ξ varies between zero for pure $s=0$ and unity for pure $s=1$, while ϵ is zero for formation with only the lowest l value, and is infinite for formation with pure $l+2$. The spin of the first excited state of ^{29}Si is $\frac{3}{2}$; thus exit channel spins are 1 and 2. The second excited state has $J=\frac{5}{2}$, and the possible exit channel spins are 2 and 3. Both channel spin and l mixing may occur simultaneously in the inelastic channels. For the n th inelastic group we define the channel spin mixing as

$$\xi_n = \sum_l \Gamma_{p_n,s_>,l} / \Gamma_{p_n}, \quad (3)$$

where $s_>$ is the higher channel spin and Γ_{p_n} is the total inelastic width in the n th channel. The two exit l mixing ratios are defined as

$$\epsilon_n(s) = \pm [\Gamma_{p_n,s,l+2} / \Gamma_{p_n,s,l}]^{1/2}. \quad (4)$$

Note that l mixing is a coherent process while channel spin mixing is incoherent.¹⁶

The data were fit utilizing our group's R matrix¹⁷ based computer program. Spins up to $J=6$ and l values up to 4 were considered in the analysis. Higher l 's are ruled out by Wigner limit considerations. The capture channel is usually insignificant and was neglected in the analysis. With the aid of shape analysis and the (p,p') angular distributions, l values were determined for almost all of the resonances. A best visual fit to the data was obtained by varying the spin J , resonance energy E_0 , and the magnitudes and phases of the allowed reduced width amplitudes which contribute to a resonance of given J . The resolution width was determined by fitting resonances with widths smaller than the experimental resolution. The shape of the resolution function was approximated by a Gaussian, with a low energy

Lorentzian tail to reproduce beam straggling effects.

The (p,p) , (p,p_1) , and (p,p_2) groups and parameters for all 66 resonances were included in the final fit. For very small resonances the J values were indefinite, but l assignments were made for all but one of the resonances observed. Provided the resonance is sufficiently large, the channel spin mixing and l mixing can usually be determined. An example of channel spin mixing is given in Fig. 1. The fits with pure channel spins are shown with the data and best fit. The lower cross section of the best fit is a result of channel spin cross terms in the expression for the differential scattering cross section.

Since l mixing is coherent, in principle, it is possible to determine the relative phases of the amplitudes for the two partial waves. In practice, few resonances were observed for which the higher partial wave contributed more than expected from penetrabilities; thus only an upper limit could normally be placed on the mixing. At the higher energies, where greater mixing is expected, overlapping levels make determination of l mixing less certain. In Fig. 2 the best fit for the l mixed, $J^\pi=1^+$ resonance at $E_p=2.96$ MeV has the same relative phase for the $l=0$ and 2 reduced width amplitudes, while the fit for opposite relative phases is obviously much poorer. Shape analysis determines the predominant l value for resonances for which mixing is not appreciable.

Inclusion of the relative phases of interfering resonances was essential to obtain good fits in all channels in the regions with many overlapping resonances. Coherent level-level interference between the broad 1^- states was observed in the elastic chan-

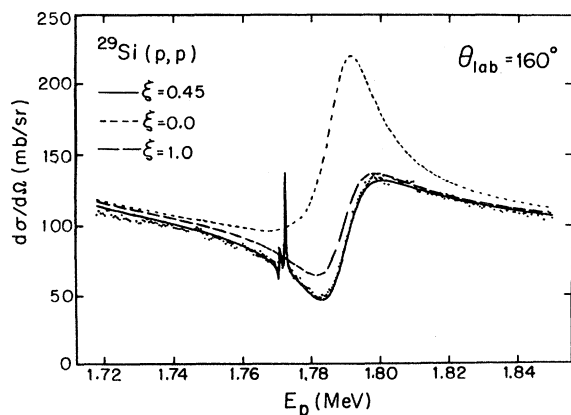


FIG. 1. The excitation function and best R -matrix fit with a channel spin mixing ratio of 0.45 for the $J^\pi=1^-$ resonance at $E_p=1.79$ MeV. The fits for pure channel spins are much poorer. For clarity the two small resonances near $E_p=1.77$ MeV have been omitted from the fits with pure channel spins.

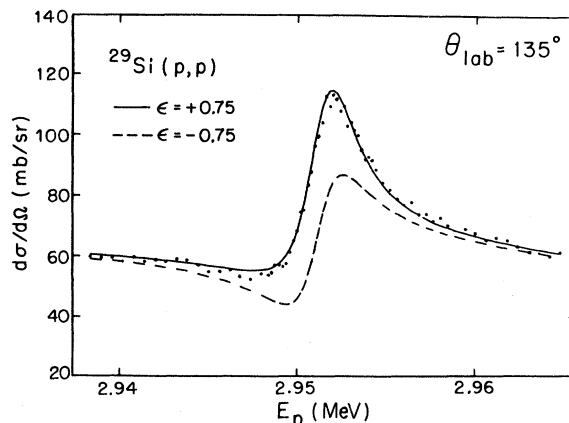


FIG. 2. The excitation function and R -matrix fits for the l mixed, $J^\pi=1^+$ resonance near $E_p=2.95$ MeV. The best fit was obtained with the same relative phase for the reduced width amplitudes of the two l values.

nel as well as for other resonances in the inelastic channels.

The fits in the region from 1.29 to 2.55 MeV were very good and the procedure here was to normalize the data to the fit; the fit included parameters of all resonances. Above 2.55 MeV the higher level density with broad overlapping levels made proper normalization more difficult. Thus the data normalization was fixed at the previously determined value, except when corrections were necessary for yield changes due to replacement of the target. Since the presence of the broad 0^- levels in this region was not apparent until all of the other levels had been fit, this normalization procedure was important. Note that although the cross sections above 2 MeV are very different from Rutherford, they are well reproduced by the inclusion of all of the observed levels and of Rutherford and hard sphere scattering.

IV. RESULTS

The four angle excitation functions are shown in Figs. 3 and 4. The solid line is the R -matrix fit to the data. The extracted resonance parameters are listed in Tables I and II. Total reduced widths γ_p^2 are defined as

$$\gamma_{p_n}^2 = \sum_{s,l} \Gamma_{p_n,s,l} / 2P_l, \quad (5)$$

where the Coulomb penetrability, P_l , is calculated from the Coulomb wave functions evaluated at a channel radius $R_c=1.25(1+A^{1/3})$ fm.

Qualitatively the agreement with previous data is fairly good. Of the 15 resonances seen in the (p,γ) reaction¹⁸ in the range $E_p=1.1-1.8$ MeV, three

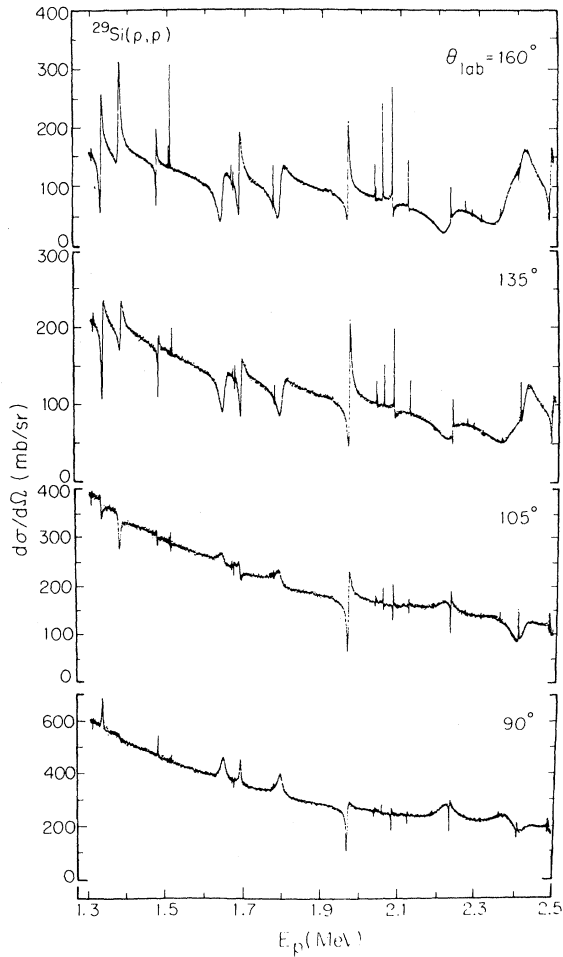


FIG. 3. The $^{29}\text{Si}(p,p)$ differential cross section for the region $E_p = 1.29$ to 2.50 MeV at four angles. The solid line is the R -matrix fit to the data.

have not been observed in elastic scattering. These are located at $E_p = 1.324$, 1.746 , and 1.749 MeV. Spin assignments below $E_p = 1.8$ MeV agree with previous results; however, the resonance at 1.302 MeV has unnatural parity¹ and is thus assigned $J=1$.

In general, the resonance energies of Poirier *et al.* are higher than those of the present measurement, with the difference increasing with energy to a maximum of about 5 keV. Other major differences are the following: (1) The 1.506 MeV, 4^- doublet of Poirier *et al.* appears as a single resonance. This energy region was remeasured several times with good statistics and with better resolution than in the previous measurement. For example, this is evident from our observation of the small f -wave resonance at 1.502 MeV which was very poorly resolved in the previous experiment. No doublet structure was observed. (2) The resonances at 1.7691 and 1.7708

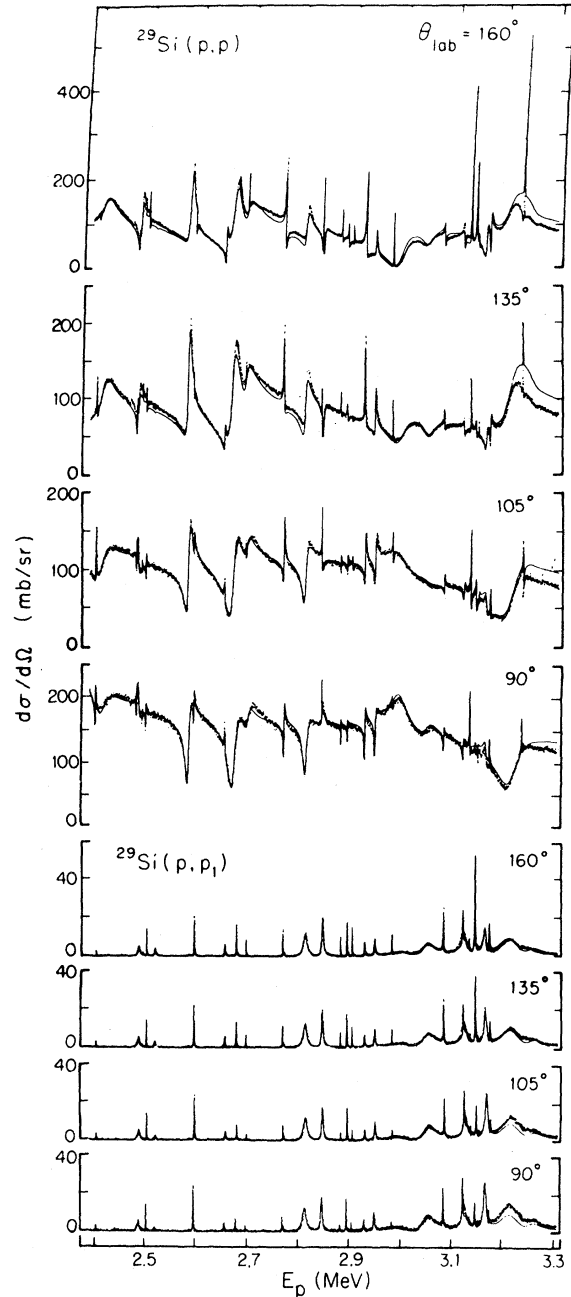


FIG. 4. The $^{29}\text{Si}(p,p)$ and (p,p_1) differential cross sections for the region $E_p = 2.39$ to 3.31 MeV at four angles. The solid line is the R -matrix fit to the data.

MeV were not observed in earlier elastic scattering measurements. (3) Three new levels were observed at 2.0336 , 2.2659 , and 2.2829 MeV. (4) The 2.2275 MeV level was assigned $J=1$ rather than $J=0$. (5) No evidence was seen for the 2.337 MeV, 0^+ resonance with a reported width of 15 keV. Also in this region the energies of the resonances at 2.3771 and 2.3588 MeV were 8 keV higher than the previous re-

TABLE I. The $^{29}\text{Si}(p,p)$ and $^{29}\text{Si}(p,p_1)$ resonance parameters.

E_p^a (MeV)	$J^{\pi b}$	l^c	ξ	ϵ	Γ_p^d (keV)	γ_p^{2e} (keV)	l_1	ξ_1	ϵ_1^f	$\Gamma_{p_1}^d$ (keV)	$\gamma_{p_1}^{2e}$ (keV)
1.3020	(0,1) ⁺	0			0.025	0.43					
1.3268	2 ⁻	1		0.0	3.1	150.0					
1.3737	1 ⁻	1	0.0		5.4	220.0					
1.4709	2 ⁻	1		0.0	0.70	20.0					
1.5023	(2,3,4) ⁻	3	1.0		0.020	67.0					
1.5060	4 ⁻	3			0.045	150.0					
1.6393	1 ⁻	1	0.5		15.0	250.0					
1.6639	2,(1) ⁺	2	1.0		0.030	3.3					
1.6685	0 ⁺	0			0.16	0.86					
1.6844	2 ⁻	1		0.0	4.50	65.0					
1.7698	1 ⁻	1	1.0		0.11	1.2					
1.7715	2,(4) ⁻	3		∞	0.045	50.0					
1.7881	1 ⁻	1	0.45		16.5	179.0					
1.9637	1 ⁺	0		0.0	3.5	10.0					
2.0336	3,(1) ⁺	2		0.0	0.040	1.5					
2.0361	(1,2,3) ⁺	2	1.0		0.040	1.5					
2.0535	2 ⁻	3		∞	0.17	75.0					
2.0789	3 ⁺	2		0.0	0.23	7.50	2	1.0	0.0	0.015	380.0
2.1203	3 ⁺	2		0.0	0.065	1.9					
2.2223	1 ⁻	1	0.55		52.0	230.0					
2.2294	1 ⁺	0		0.0	0.53	1.0					
2.2679	(2,3,4) ⁻	3	1.0		0.017	4.1					
2.2849	(2,3,4) ⁻	3	1.0		0.010	2.3					
2.3095	(2,3) ⁻	3	1.0		0.050	11.0	1	0.0	0.0	0.4	120.0
2.3588	4 ⁻	3			0.015	2.9					
2.3771	2 ⁻	1		0.0	70.0	240.0					
2.4063	2 ⁺	2	1.0		0.38	6.1	0 ^g		0.0	0.02	1.0
2.4183	0 ⁺	0			28.0	41.0					
2.4866	0 ⁺	0			1.0	1.4					
2.4901	1 ⁻	1	0.98		4.3	12.0	1	0.85	0.0	0.35	37.0
2.4979	(1,2,3) ⁺	2	1.0		0.65	0.88	0 ^g		0.0	0.002	0.060
2.5056	2 ⁺	2	0.0		0.16	2.1	0 ^g		0.0	0.11	3.2
2.5221	2,(1) ⁻	1	1.0	0.0	0.05	0.14	1	0.0	0.0	2.2	200.0
2.5881	1 ⁺	0		0.0	7.4	9.1					
2.5992	2 ⁺	2	1.0		0.32	3.6	0		-0.50	0.75	94.0
2.6602	1 ⁻	1	1.0		1.7	3.9	1	0.5	0.0	0.18	8.6
2.6761	1 ⁺	0		0.0	18.0	20.0					
2.6826	3 ⁻	3	1.0		0.70	6.5	1	1.0	0.0	0.60	26.0
2.7019	4 ⁻	3			0.040	3.6	3	h		0.010	61.0
2.7027	0 ⁺	0			13.0	14.0					
2.7057	0 ⁻	1			30.0	65.0					
2.7745	2 ⁻	3		∞	0.060	4.6	1	0.30	0.0	0.26	7.9
2.7766	2 ⁺	2	0.80		1.3	11.0	0		0.0	0.030	0.30
2.8188	1 ⁺	0		-0.30	6.0	9.5	0 ^g		0.0	2.7	24.0
2.8509	4 ⁻	3			0.17	11.0	3	h		0.002	6.0
2.8529	2 ⁻	1		0.0	2.4	4.4	1	0.35	0.0	1.0	24.0
2.8886	3 ⁺	2		0.0	0.10	0.72	2	1.0	0.0	0.020	3.1
2.9014	2 ⁺	2	0.20		0.24	1.7	0		0.0	0.40	2.7
2.9115	3 ⁻	3	0.0		0.040	2.4	1		0.0	0.060	1.1
2.9361	2 ⁺	2	0.30		1.3	8.7	0		0.0	0.10	0.62
2.9562	1 ⁺	0		0.75	2.3	6.5	2	0.5	∞	0.60	73.0
2.9902	4 ⁻	3			0.10	5.2	3	h		0.016	27.0
3.0042	1 ⁻	1	0.70		37.0	58.0	1	0.0	0.0	2.0	29.0
3.0253	0 ⁻	1			200.0	300.0					

TABLE I. (Continued.)

E_p^a (MeV)	$J^\pi{}^b$	l^c	ξ	ϵ	Γ_p^d (keV)	γ_p^{2e} (keV)	l_1	ξ_1	ϵ_1^f	$\Gamma_{p_1}^d$ (keV)	$\gamma_{p_1}^{2e}$ (keV)
3.0656	1 ⁻	1	0.20		25.0	37.0	1	0.5	0.0	4.4	54.0
3.0914	2 ⁺	2	0.90		0.50	2.7	0		0.0	0.60	2.6
3.1299	2 ⁺	2	0.0		0.60	3.1	0	1.0	-0.33	1.0	10.0
3.1379	1 ⁺	2		∞	3.0	15.0	0 ^g		0.0	15.0	58.0
3.1432	4 ⁻	3			0.45	18.0	3	h		0.010	9.4
3.1537	3 ⁻	1	0.20		0.60	23.0	1		0.0	0.50	4.9
3.1594	2 ⁺	2	1.0		0.12	0.60	0		0.0	0.020	0.070
3.1741	2 ⁻	1		0.0	4.0	5.4	1	0.95	0.0	1.8	17.0
3.1821	2 ⁻	1		0.0	1.5	2.0	1	0.30	0.0	0.14	1.3
3.2224	1 ⁺	0		0.50	38.0	59.0	0 ^g	0.20	i	10.0	130.0
3.2451	4 ⁻	3			0.30	10.0					
3.2656	(1 ⁺)	2			3.0	13.0	0 ^g		0.0	30.0	90.0

^aLaboratory energies are quoted. The absolute energies should be accurate within 3 keV. Except for very large resonances, the relative energies over a small energy range should be accurate within a few hundred eV.

^bSpin assignments have been listed according to the following convention: 0⁺ definite spin and parity; 1,(0)⁺ definite l value, with the preferred spin outside of parentheses; (0,1)⁺ definite l value, spin not completely determined; (0⁺) possible l value and J^π .

^cFor ϵ infinite the higher l value is listed.

^dIf several spins are listed, the widths and mixing ratios are given for the first spin listed.

^eTotal reduced widths corresponding to the total laboratory widths listed are calculated according to Eq. (5).

^fExcept as noted, simultaneous channel spin mixing and l mixing were not observed.

^gParameters quoted for inelastic decay are for the lowest possible l values in ambiguous cases.

^hThe exit channel spin is undetermined.

ⁱ $\epsilon_1(1)=0.0$, $\epsilon_1(2)$ infinite.

sults. (6) Significantly lower channel spin mixing ratios were previously assigned for the $J^\pi=1^-$ states at 2.222 and 2.490 MeV. (7) Widths for eight resonances varied more than 30% from the present values. The less comprehensive analysis and poorer resolution probably account for most of these differences.

The comparison with the data and analysis of Hemsley *et al.* is also qualitatively good with the following exceptions: (1) The 2.8474 MeV resonance was assigned $J=2$ instead of $J=4$. (2) The resonance at 2.9802 MeV has $l=3$, not $l=4$. (3) The channel spin mixing ratios previously assigned for the resonances at 2.5056, 2.6602, and 2.8529 MeV are very different from those in this work. (4) The l mixing ratios for the states at 2.5881 and 2.6761 were nonzero in the previous analysis. (5) Almost all of the widths differed some 30 to 60% from the present results. These discrepancies can be attributed to our improved treatment of resonance interference, better normalization procedures, and more precise treatment of the inelastic widths. Some 23 resonances analyzed in the present study were omitted in the previous analyses.

The errors associated with the fit parameters list-

ed in Tables I and II have been estimated by examining the range over which each parameter could be varied without appreciably degrading the fit. Below 2.7 MeV the errors were smaller than in the complicated higher energy regions. As a guide the errors in the widths are 10% below 2.7 MeV and 20% above 2.7 MeV. Typical errors in the channel spin mixing ratios are 8% below 2.7 MeV and 15% above this energy, while the errors in the l mixing ratios are 10% for small isolated resonances and up to 30% for the broad overlapping resonances.

V. ANALOG STATES

Five analogs have previously been identified in our energy range.¹ The analogs of states in ^{30}Si at $E_x=6.503$, 6.537, 6.641 (doublet), and 6.744 MeV have been identified as the resonances in ^{30}P at $E_p=1.506$, 1.664, 1.669, 1.684, and 1.788 MeV, with $J^\pi=4^-$, 2⁺, 0⁺, 2⁻, and 1⁻, respectively. Our results are consistent with these assignments. In addition, the analogs of the 2⁻ state at $E_x=7.508$ MeV and the 1⁻ state at 8.163 MeV are identified as the resonances at $E_p=2.377$ MeV and the doublet around 3.003 MeV.

TABLE II. The $^{29}\text{Si}(p,p_2)$ resonance parameters.

E_p^a (MeV)	J^π	l_2	ξ_2	ϵ_2	Γ_{p_2} (keV)	$\gamma_{p_2}^2$ (keV)
3.1299	2^+	0		0.0	0.15	10.0
3.1432	4^-	1		0.0	0.080	18.0
3.1537	3^-	1	1.0	0.0	0.20	42.0
3.1594	2^+	0		0.0	0.18	10.0
3.1741	2^-	1	0.0	0.0	0.50	93.0
3.1821	2^-	1	0.0	0.0	0.50	89.0
3.2451	4^-	1		0.0	0.010	1.2

^aConventions are the same as in Table I.

Identification of analog states is made on the basis of angular momentum, energy, and strength. An estimate of the analog state energy is obtained with the aid of an approximate value of the Coulomb displacement energy and the relation

$$E_C = B_n + E_p^{\text{c.m.}} - E_x,$$

where E_C is the Coulomb displacement energy, B_n is the binding energy of the last neutron in the parent nucleus, $E_p^{\text{c.m.}}$ is the center of mass energy of the analog resonance, and E_x is the excitation energy of the parent state. E_C was calculated with the value¹⁹ $B_n = 10.610$ MeV. Strengths may be compared through the spectroscopic factors, the direct reaction spectroscopic factor S_{dp} , and the analog spectroscopic factor

$$S_p = (2T_0 + 1)\Gamma_p / \Gamma_{sp},$$

where T_0 is the isospin of the target nucleus, Γ_p is the analog laboratory width, and Γ_{sp} is the proton single particle width. Values of Γ_{sp} were calculated with the methods described by Harney and Weidenmüller.²⁰

For nuclei with very low level densities analogs occur as individual states. For nuclei with high level densities analogs are fragmented, and are normally strongly enhanced with respect to the background states. In either case identification is a simple process. However, there are intermediate situations where the identification process is not as clear, and for which quantitative strength comparisons are not very meaningful. Some of the analogs in the present measurement appear to fall into this latter class. To aid in the discussion of analog identification, the reduced widths are plotted in Fig. 5 for resonances with $J^\pi = 0^+, 1^-, 2^+, 2^-$ (with $l=1$), and 4^- . Analog parameters are listed in Table III.

Arguments for identification of analog states are as follows:

1. $J^\pi = 4^-$. A strong analog is expected near $E_p = 1.5$ MeV and is observed as a single resonance.

The spectroscopic factors are in agreement. Other $l=3$ strength has been observed in the (d,p) reaction but no definite J values have been assigned.

2. $J^\pi = 1^-$. Strong analogs are expected near $E_p = 1.7$ and 3.0 MeV. Since there is a very large concentration of strength in the region of the lower analog state, no realistic value of the analog state strength can be obtained. Most of the analog strength lies in the state at $E_p = 1.788$ MeV, al-

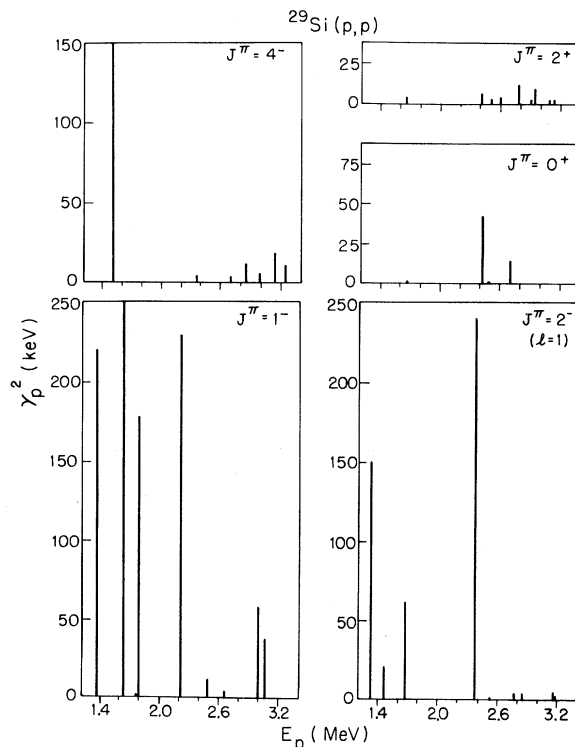


FIG. 5. Reduced widths for $^{29}\text{Si}(p,p)$ for $J^\pi = 1^-, 2^-$ ($l=1$ only), 4^- , 0^+ , and 2^+ . Analogs observed are the 1^- state at 1.79 MeV, the 1^- doublet near 3.02 MeV, the 2^- states at 1.68 and 2.38 MeV, and the 4^- state at 1.51 MeV. The 0^+ states near 1.67 and 2.42 MeV and the 2^+ state at 1.66 MeV are probably analogs.

TABLE III. Analog state parameters.

J^π	E_x^a (MeV)	l	E_p^{lab} (MeV)	E_C (MeV)	Γ_{sp}^b (keV)	Γ_p (keV)	S_p	S_{dp}^c
4^-	6.503	3	1.506	5.566	0.21	0.045	0.43	0.43
2^+	6.537	2	1.664	5.682	2.9	0.030	0.01	
0^+	6.641	0	1.669	5.582	59.0	0.16	0.003	
2^-	6.641	1	1.684	5.597	54.0	4.5	0.17	0.09
1^-	6.744	1	1.788	5.594	50.0	16.5	0.66	0.33
2^-	7.508	1	2.377	5.400	230.0	70.0	0.61	0.34
1^-	8.163	1	3.025	5.352	476.0	62.0	0.26	0.23

^aExcitation energies in ^{30}Si from Ref. 1.

^bValues of Γ_{sp} are averaged over $n=1$ and 2 for $J=2$, and also over $j=\frac{1}{2}$ and $\frac{3}{2}$ for $J=1$.

^cSpectroscopic factors from Ref. 1.

though γ decay of the resonance at $E_p = 1.639$ MeV demonstrates isospin mixing.¹ The strength for the higher analog may be reliable. There are several additional complications. The states excited by $l=1$ transfer in this mass region may have principal quantum numbers $n=1$ or 2 , and for $J=1$, can have particle angular momenta $j=\frac{1}{2}$ and $\frac{3}{2}$. The stripping reaction determines neither n nor j . The resonance reaction determines two possible solutions for the relative j contribution. Fortunately, the value of Γ_{sp} is not very sensitive to these changes; we use an average value of Γ_{sp} . The spectroscopic factor for the lower 1^- analog does not agree with the (d,p) value, while the spectroscopic factor for the upper analog agrees.

3. $J^\pi=2^-$. Analogs are expected near $E_p=1.7$ and 2.4 MeV. Since there are background states with comparable strength, especially for the lower analog, strength comparisons are not expected to be significant. The spectroscopic factors disagree for both analogs.

4. $J^\pi=0^+$. The 0^+ resonance at $E_p=1.6685$ has been identified as the analog of the ^{30}Si state at $E_x=6.641$ MeV. The 0^+ level at $E_x=7.44$ MeV in ^{30}Si could correspond to one of the 0^+ resonances observed. There are no (d,p) spectroscopic factors for these states.

5. $J^\pi=2^+$. One very weak state at $E_p=1.6639$ MeV has been identified as the analog of the 6.537 MeV state in ^{30}Si . There are several other 2^+ states in ^{30}Si which would correspond to weak analog resonances. Several 2^+ resonances are observed, but it is not possible to make definite assignments.

The analog state results are in reasonable agreement with previous assignments. The analog spectroscopic factors for the lower energy 1^- resonance

and the 2^- resonances are larger than the (d,p) spectroscopic factors. This is surprising since for analog states in $1f-2p$ shell nuclei the analog spectroscopic factors were systematically lower than the (d,p) values.¹² However, values of S_p greater than S_{dp} have been previously observed in the $^{27}\text{Al}-^{27}\text{Mg}$ isobaric pair.¹¹ In the present case, mixing of the large background strength with the analog states probably accounts for most of these discrepancies.

VI. SUMMARY

Differential cross sections were measured for the $^{29}\text{Si}(p,p)$, (p,p_1) , and (p,p_2) reactions from $E_p=1.29$ MeV for (p,p) , 2.40 MeV for (p,p_1) , and 3.09 MeV for (p,p_2) to 3.31 MeV. Resonance parameters were extracted for 66 resonances with an R -matrix analysis code. Several analogs were identified and Coulomb energies and spectroscopic factors obtained.

The major importance of these results is the demonstration that, in spite of additional analysis complications, excellent overall fits can be obtained, and channel spin mixing parameters and l mixing parameters can be well determined. High resolution experiments on other odd-mass targets in this mass region are now in progress.

ACKNOWLEDGMENTS

The authors would like to thank Professor P. M. Endt for advice and suggestions, and B. H. Chou, K. B. Sales, K. M. Whatley, and J. F. Shriner, Jr. for assistance in performing the experiment. This work was supported in part by the U.S. Department of Energy.

- ¹P. M. Endt and C. Van der Leun, Nucl. Phys. A310, 1 (1978).
- ²J. M. Pearson and A. Richter, Phys. Lett. 56B, 112 (1975).
- ³H. Driller, E. Blanke, H. Genz, A. Richter, G. Schrieder, and J. M. Pearson, Nucl. Phys. A317, 300 (1979).
- ⁴O. P. Sushkov and V. V. Flambaum, Pis'ma Zh. Eksp. Teor. Fiz. 32, 377 (1980) [JETP Lett. 32, 352 (1980)].
- ⁵V. P. Alfimenkov, S. B. Borzakov, Vo Van Thuan, Yu. D. Mareev, L. B. Pikelner, A. S. Khrykin, and E. I. Sharapov, Proceedings of the International Conference on Nuclear Data for Science and Technology, Antwerp, 1982 (unpublished).
- ⁶F. C. Barker and N. Ferdous, J. Phys. G 7, 1239 (1981).
- ⁷V. E. Storizhko and A. I. Popov, Izv. Akad. Nauk SSSR, Ser. Fiz. 28, 1152 (1964) [Bull. Acad. Sci. USSR, Phys. Ser. 28, 1054 (1965)].
- ⁸A. N. L'vov, A. E. Popov, P. V. Sorokin, and V. E. Storizhko, Izv. Akad. Nauk SSSR, Ser. Fiz. 30, 439 (1966) [Bull. Acad. Sci. USSR, Phys. Ser. 30, 447 (1966)].
- ⁹C. P. Poirier, J. Walinga, J. C. Manthuruthil, and G. I. Harris, Phys. Rev. C 1, 1982 (1970).
- ¹⁰J. W. Hensky, S. C. Ling, and P. J. Wolfe, Phys. Rev. C 8, 192 (1973).
- ¹¹C. R. Westerfeldt, G. E. Mitchell, E. G. Bilpuch, and D. A. Outlaw, Nucl. Phys. A303, 111 (1978).
- ¹²E. G. Bilpuch, A. M. Lane, G. E. Mitchell, and J. D. Moses, Phys. Rep. 28, 145 (1976).
- ¹³J. B. Marion, Rev. Mod. Phys. 38, 660 (1966).
- ¹⁴J. Vorona, J. W. Olness, W. Haeberli, and H. W. Lewis, Phys. Rev. 116, 1563 (1959).
- ¹⁵D. A. Outlaw, G. E. Mitchell, and E. G. Bilpuch, Nucl. Phys. A269, 99 (1976).
- ¹⁶A. A. Kraus, Jr., J. P. Schiffer, F. W. Prosser, Jr., and L. C. Biedenharn, Phys. Rev. 104, 1667 (1956).
- ¹⁷A. M. Lane and R. G. Thomas, Rev. Mod. Phys. 30, 257 (1958).
- ¹⁸G. I. Harris, A. K. Hyder, Jr., and J. Walinga, Phys. Rev. 187, 1413 (1969).
- ¹⁹A. H. Wapstra and K. Bos, At. Data Nucl. Data Tables 19, 217 (1977).
- ²⁰H. L. Harney and H. A. Weidenmüller, Nucl. Phys. A139, 241 (1969).